

Context-Based Semantic-Aware Alignment for Semi-Supervised Multi-Label Learning

Heng-Bo Fan^{1*} Ming-Kun Xie^{1*} Jia-Hao Xiao¹ Sheng-Jun Huang^{1†}

¹Nanjing University of Aeronautics and Astronautics, Nanjing, China

{fan.heng_bo, mkxie, jiahaoxiao, huangsj}@nuaa.edu.cn

Abstract

Due to the lack of extensive precisely-annotated multi-label data in real word, semi-supervised multi-label learning (SSMLL) has gradually gained attention. Abundant knowledge embedded in vision-language models (VLMs) pre-trained on large-scale image-text pairs could alleviate the challenge of limited labeled data under SSMLL setting. Despite existing methods based on fine-tuning VLMs have achieved advances in weakly-supervised multi-label learning, they failed to fully leverage the information from labeled data to enhance the learning of unlabeled data. In this paper, we propose a context-based semantic-aware alignment method to solve the SSMLL problem by leveraging the knowledge of VLMs. To address the challenge of handling multiple semantics within an image, we introduce a novel framework design to extract label-specific image features. This design allows us to achieve a more compact alignment between text features and label-specific image features, leading the model to generate high-quality pseudo-labels. To incorporate the model with comprehensive understanding of image, we design a semi-supervised context identification auxiliary task to enhance the feature representation by capturing co-occurrence information. Extensive experiments on multiple benchmark datasets demonstrate the effectiveness of our proposed method.

1. Introduction

In contrast to traditional multi-class classification, which assumes that each instance belongs to a single class, multi-label learning (MLL) aligns more closely with real-world scenarios where each image may contain multiple semantic objects simultaneously. This complexity arises from diverse shapes and sizes of objects contained in an image, making MLL a particularly challenging task. Thanks to the powerful capacity of deep neural networks (DNNs), MLL has

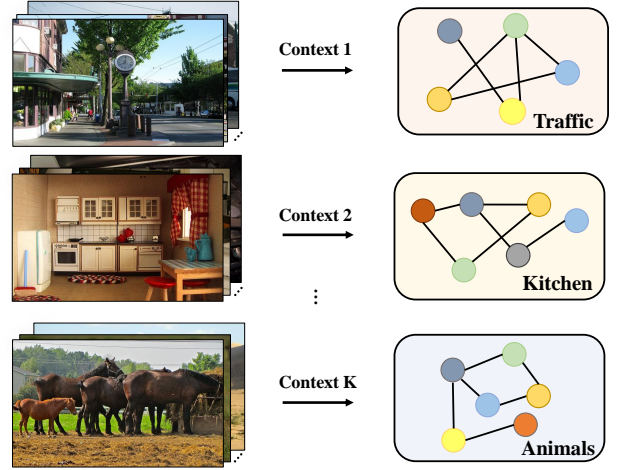


Figure 1. In MLL, context information determines the co-occurrence relationships among categories. Semantics belonging to the same context are more likely to appear simultaneously. To leverage this, we introduce an auxiliary task: Context Identification, during model training. This task helps narrow down the label space into its relevant subset.

achieved significant success in various domains, *e.g.*, video annotation [20], the recommendation system [1, 24], and medical diagnosis [2, 13].

While multi-label learning (MLL) has recently made significant strides, a potential challenge lies in the fact that training an effective DNN often demands extensive, accurately-annotated multi-label data, which can be difficult and costly to collect in real world. Semi-supervised multi-label learning (SSMLL) provides a solution to this problem by training a MLL model based on a limited set of labeled examples with a substantial amount of unlabeled examples.

Recently, vision-language models (VLMs) have made significant progress in various fields, benefiting from their pre-training on large-scale datasets consisting of image-text pairs. This motivates us to leverage the abundant knowledge embedded in VLMs to alleviate the challenge of limited la-

*Equal contributions.

†Corresponding author.

beled data. Several efforts have been made to incorporate VLMs into multi-label learning with partial labeling [9, 34], yielding promising results in this task. Unfortunately, since these methods are not specifically designed for SSMLL, they cannot fully leverage the precisely-labeled examples to enhance the learning process on unlabeled data, resulting in sub-optimal performance. To the best of our knowledge, in this paper, we make the first attempt to fine-tune VLMs in SSMLL downstream task, which aims to leverage the information of unlabeled data and the knowledge embedded in VLMs simultaneously.

One of the primary challenges in Multi-Label Learning (MLL) lies in exploring the correlations among labels. Existing methods often capture label correlations by either adopting graph convolutional network [6] or developing label masking strategy [41]. In practice, we observe that whether a target is present in an image often depends on the context of the image. For example, as shown in Figure 1, an image captured in a street scene is more likely to contain objects such as *car*, *people*, or *traffic light*; whereas in an image taken in a kitchen, it is more probable to have objects like *refrigerator*, *oven*, or *dining table*. In other words, the co-occurrence of these labels constitutes the context. This motivates us to identify image contexts to capture co-occurrence relationships, thereby enhancing the performance of SSMLL.

In this paper, we propose a context-based semantic-aware alignment method to solve the SSMLL problem, which aims to improve pseudo-labeling performance by leveraging the knowledge of CLIP. On the one hand, we develop the semantic-aware alignment target task to encourage a more compact alignment between text features and image features. The core idea involves aligning text features with label-specific features, rather than features of the entire image. This simplifies the alignment task, contributing to a more effective utilization of knowledge embedded in CLIP. On the other hand, we design a context identification auxiliary task to explore co-occurrence information. We first divide the original dataset into multiple clusters, each representing a context category; then, we formulate the context identification task as a semi-supervised learning problem to leverage the co-occurrence relationships. Experimental results on multiple benchmark datasets demonstrate that our method outperforms existing fine-tuning methods.

2. Related Work

2.1. Multi-label Learning

Multi-label learning has experienced rapid development in recent years. And these works can be mainly classified into three groups. The first group attempted to capture the correlation between labels using graph-based [2, 6] methods, RNN/LTSM [37, 42], or transformer [25, 43]. Correlation between different labels can be used as prior knowledge for

classification task. The second group improved loss function [14, 18, 21, 28] to alleviate the problem of extreme imbalance ratio between positive and negative labels. The final group designed more sophisticated model structures to better extract local image feature using attention-based [22, 33] technique.

Due to limited annotations in real-world scenario, more realistic problem settings have been proposed in MLL. For instance, *partial label* [38, 39] setting, where a subset of original labels is available for each training instance. *Single positive label* [8] setting is a more extreme case where merely one single positive label is provided for every instance. However, the field of SSMLL is relatively unvisited. Wang *et al.* [35] and Zhao *et al.* [47] leveraged label relations in non-deep scenario, which cannot be applied to our case. Wang *et al.* [36] used two classifier to deal with the features of labeled and unlabeled samples separately, which could reduce the distribution gap between these two datasets. However, due to the extreme limited supervised information in SSMLL, previous methods failed to generate accurate pseudo-labels. Thus, in this paper, we leverage VLMs pre-trained on numerous image-text pairs to alleviate the challenge of limited labeled data.

2.2. Overview of CLIP

VLMs have achieved tremendous success in various fields in recent years. As a milestone of VLMs, CLIP, pre-trained with 400 million image-text pairs, consists of an image encoder and a text encoder. The optimizing objective of CLIP is to align visual and textual modalities in latent space using a contrastive loss. Benefited from the tight alignment of two modalities, CLIP has exhibited promising result on classification tasks simply by using prompt as query. One naive way to construct prompt is using a template like "a photo of a [CLS].", where [CLS] can be substituted with real category names. [48] has demonstrated that optimizing continuous learnable prompt \mathbf{V} rather than using hand-crafted ones could achieve better performance on different tasks. Given an image input \mathbf{x}_i , the two modal features can be computed as follows

$$\mathbf{h}_i = \text{Enc}_I(\mathbf{x}_i), \mathbf{w} = \text{Enc}_T(\mathbf{V}), \quad (1)$$

and then CLIP computes cosine similarity between image feature \mathbf{h}_i and text feature \mathbf{w} . Finally we optimize learnable prompts by maximizing model's prediction on ground-truth label

$$p(y|\mathbf{x}_i) = \frac{\exp(\langle \mathbf{h}_i, \mathbf{w} \rangle / \tau)}{\sum_{j=1}^C \exp(\langle \mathbf{h}_i, \mathbf{w}_j \rangle / \tau)}, \quad (2)$$

where $\langle \cdot, \cdot \rangle$ compute cosine similarity and τ is a temperature parameter.

Follow-up works introduced various prompt designs like adding prompts to visual modality [12, 19, 30, 31, 46],

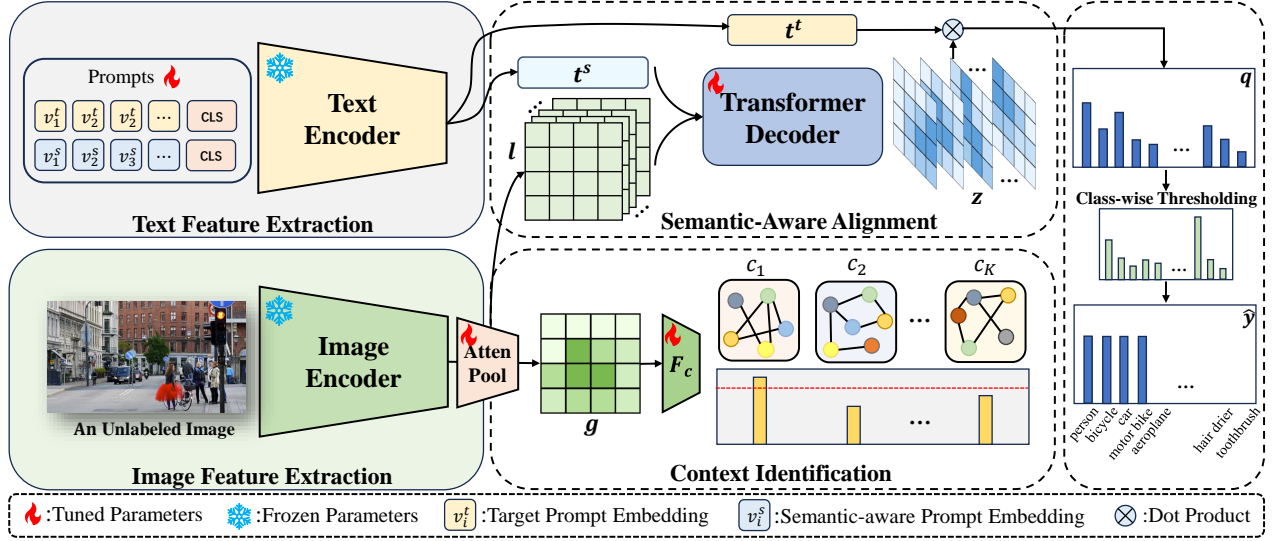


Figure 2. An overview of our proposed method. We begin by employing CLIP to extract both image features and C -class text features. Subsequently, we thoroughly leverage the pre-training knowledge embedded in the text encoder of CLIP to extract label-specific image features. To further exploit label correlation, we introduce a **Context Identification** task. Finally, we optimize the network by generating pseudo-labels with class-wise thresholds.

or using multiple prompts simultaneously [15, 34]. More adapter designs [11, 27, 44, 45] have been proposed to further increase CLIP’s transfer ability on downstream task. While its powerful generalization ability on partial multi-label learning [34] and zero-shot multi-label learning [9] have been validated, adapting CLIP into SSMLL is still unexplored. Furthermore, these approaches failed to consider the unique challenge of multi-label learning, and fine-tuned CLIP by aligning multiple class text embeddings with one single image embedding. This results in sub-optimal model performance due to its complex optimization objective. Therefore, we propose to simplify the alignment task and fully leverage contextual information within an image to enhance the quality of pseudo labels. This results in a more compact alignment between visual and textual modalities, providing a solution to SSMLL problem.

3. Proposed Method

In this section, we present Context-Based Semantic-Aware Alignment framework to adapt CLIP to SSMLL. We use $\mathbf{x} \in \mathcal{X}$ to denote an image, and $\mathbf{y} \in \mathcal{Y}$ to denote its label, where $\mathcal{X} \in \mathbb{R}^d$ represents the feature space and $\mathcal{Y} \in \{0, 1\}^C$ represents the label space. Under the SSMLL problem setting, the whole training dataset can be divided into a labeled dataset $\mathcal{D}_l = \{(\mathbf{x}_i, \mathbf{y}_i)\}_{i=1}^m$ and an unlabeled dataset $\mathcal{D}_u = \{\mathbf{x}_j\}_{j=1}^n$. For an image $\mathbf{x}_i \in \mathcal{D}_l$, its label vector \mathbf{y}_i is a multi-hot vector, where $y_{ik} = 1$ indicates the presence of object k in image \mathbf{x}_i , while $y_{ik} = 0$ indicates its absence.

The primary challenge posed by SSMLL lies in how to generate high-quality pseudo-labels for unlabeled instances based on a small number of labeled examples. To address this challenge, we improve the quality of pseudo-labels from two aspects: 1) develop the semantic-aware alignment target task to enforce a compact alignment between two modalities; 2) design the context identification auxiliary task to exploit co-occurrence relationships. Figure 2 illustrates the whole pipeline of our framework. Below, we will introduce the details of these two components.

3.1. Semantic-Aware Alignment

Instead of fine-tuning the entire CLIP, the existing methods [34, 48] often fine-tune the learnable prompts by aligning text features with image features. However, as shown in Figure 3, when tackling instances associated with multiple labels, it transforms the alignment task from a one-to-one task, *i.e.*, aligning one text embedding with one image embedding, into a many-to-one problem, *i.e.*, aligning multiple text embeddings with one image embedding. This often results in the sub-optimal alignment between text features and image features, leading to unfavorable fine-tuning performance. To address this problem, we propose to perform semantic-aware alignment between the text features and label-specific image features rather than the features of a whole image. This simplifies the alignment task to an one-to-one problem, leading to a better alignment between two modalities.

Specifically, for each unlabeled instance \mathbf{x}_j , by feeding

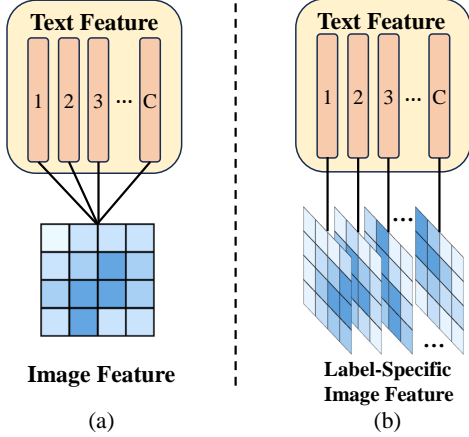


Figure 3. A comparison between previous alignment task and ours. (a) Previous methods align multiple text embeddings with one whole image embedding. Instead, (b) our method extracts label-specific image features and aligns them with the corresponding class text features.

it into the image encoder $\text{Enc}_I(\cdot)$, we obtain the image features $\mathbf{f}_j = \text{Enc}_I(\mathbf{x}_j)$. Taking ResNet [16] as an example, CLIP slightly modifies its structure by adding a attention pooling layer before taking the inner product with text feature. CLIP applies average pooling to $\mathbf{f}_j \in \mathbb{R}^{HW \times d}$ to obtain global image feature $\bar{\mathbf{f}}_j \in \mathbb{R}^{1 \times d}$, where H, W, d are the height, width and the number of channels. Then, the concatenated image features $[\bar{\mathbf{f}}_j, \mathbf{f}_j]$ is fed into a multi-head self-attention layer to obtain the global image feature \mathbf{g}_j and feature map \mathbf{l}_j :

$$[\mathbf{g}_j, \mathbf{l}_j] = \text{SelfAttention}([\bar{\mathbf{f}}_j, \mathbf{f}_j]). \quad (3)$$

In the original CLIP, only the global image \mathbf{g}_j feature is used to compute the similarity with text feature. However, we find that the feature map \mathbf{l}_j still has abundant semantics and can be used to extract label-specific features. Thus we denote \mathbf{l}_j as local image feature.

Suppose the length of learnable prompt is N , so for every class k , we use a semantic-aware prompt, $\mathbf{P}_k^s = [\mathbf{v}_1^s, \mathbf{v}_2^s, \dots, \mathbf{v}_N^s, \text{CLS}_k]$ to allocate attention on regions of interest and a target prompt $\mathbf{P}_k^t = [\mathbf{v}_1^t, \mathbf{v}_2^t, \dots, \mathbf{v}_N^t, \text{CLS}_k]$ to perform target multi-label alignment, where \mathbf{v}_j^s and \mathbf{v}_j^t are learnable word embeddings and CLS_k is the word embedding of the k -th class name. By feeding the prompts into the text encoder of CLIP $\text{Enc}_T(\cdot)$, we obtain the semantic-aware text embedding \mathbf{t}_k^s and target text embedding \mathbf{t}_k^t . We perform cross attention between $\{\mathbf{t}_k^s\}_{k=1}^C$ and \mathbf{l}_j , i.e. $\{\mathbf{t}_k^s\}_{k=1}^C$ as query, \mathbf{l}_j as key and value, to generate label-specific image features:

$$\{\mathbf{z}_k^{(j)} | k \in [C]\} = \text{TransformerDec}(\{\mathbf{t}_k^s\}_{k=1}^C, \mathbf{l}_j, \mathbf{l}_j), \quad (4)$$

where $\mathbf{z}_k^{(j)}$ is the feature of the k -th class for instance \mathbf{x}_j . Compared to the image features that encodes the information of a whole image, label-specific features capture the information of each semantic object in an image. Then, we align the target text features \mathbf{t}_k^t and label-specific image features \mathbf{z}_k in an one-to-one manner and obtain the alignment degree:

$$\mathbf{p}_j^t = [\sigma(\langle \mathbf{z}_1^{(j)}, \mathbf{t}_1^t \rangle), \dots, \sigma(\langle \mathbf{z}_C^{(j)}, \mathbf{t}_C^t \rangle)], \quad (5)$$

where $\sigma(\cdot)$ is the sigmoid function. For simplicity, we use \mathbf{q}_j^t and \mathbf{p}_j^t to denote the alignment degrees on the weakly-augmented and strongly-augmented versions of images.

Semi-Supervised Semantic-Aware Alignment. In order to leverage the information of unlabeled instances, we generate the pseudo-labels using class-distribution-aware thresholding (CAT) [40]:

$$\hat{y}_{jk} = \begin{cases} 1 & \text{if } q_{jk} \geq \tau_k^+, \\ 0 & \text{if } q_{jk} \leq \tau_k^-, \\ -1 & \text{otherwise,} \end{cases} \quad (6)$$

where τ_k^+ and τ_k^- are the class-wise thresholds that respectively capture the positive and negative proportions in the unlabeled data. Given the predicted degrees \mathbf{p}_j^t and pseudo-labels $\hat{\mathbf{y}}_j$, we define the unsupervised alignment loss as follows:

$$\mathcal{L}_{unsup} = \sum_{j=1}^n \sum_{k=1}^C L(p_{jk}^t, \hat{y}_{jk}), \quad (7)$$

here, $L(p_k, y_k) = y_k L_+(p_k) + (1 - y_k) L_-(p_k)$ is the ASL loss [28], where $L_+(p_k) = -(1 - p_k)^{\gamma_1} \log(p_k)$ and $L_-(p_k) = -(p_k)^{\gamma_2} \log(1 - p_k)$. γ_1 and γ_2 are focusing parameters to adjust focusing levels of the positive and negative examples. We define the supervised alignment loss as:

$$\mathcal{L}_{sup} = \sum_{i=1}^m \sum_{k=1}^C L(p_{ik}^t, y_{ik}). \quad (8)$$

3.2. Context Identification

It is fundamental to exploit the label correlations, which has been regarded as an essential information for MLL. Existing methods often capture label correlations by either using graph convolutional network [6] or designing label masking strategy [41]. Unlike these works, we propose to design an auxiliary task that identifies the context of an image for capturing co-occurrence information. Specifically, our approach involves partitioning the original label space into several groups, each representing a context category comprising fewer co-occurring semantic classes. Subsequently, we formulate the context identification task

as a semi-supervised classification problem to improve the learning of co-occurrence features for both labeled and unlabeled instances, aiming to enhance the performance of pseudo-labeling.

Self-Supervised Context Partition. To capture the correlations among labels, we partition the original label set into several context subsets based on label co-occurrence in a self-supervised manner. Specifically, we begin by defining a $C \times C$ co-occurrence matrix \mathbf{S} , where $S_{kl} = \frac{e_{kl}}{n_k}$. Here, e_{kl} represents the number of images containing both the k -th and l -th labels, and n_k represents the number of images containing only the k -th label. Inspired by [41], we apply spectral clustering to the co-occurrence matrix \mathbf{S} to partition the label space into several clusters. Here the affinity matrix of category graph can be computed as follows:

$$\mathbf{P} = \frac{\mathbf{S} + \mathbf{S}^T}{2}. \quad (9)$$

The context partition is then formulated as a normalized graph-cut problem:

$$\hat{\mathbf{F}} \leftarrow \arg \min_{\mathbf{F}} \text{Trace}(\mathbf{F}^T \mathbf{D}^{-\frac{1}{2}} \mathbf{L} \mathbf{D}^{-\frac{1}{2}} \mathbf{F}), \text{ s.t. } \mathbf{F}^T \mathbf{F} = \mathbf{I}, \quad (10)$$

here, \mathbf{D} is a diagonal matrix, where the diagonal element $D_{kk} = \sum_{l=1}^C S_{kl}$, and $\mathbf{L} = \mathbf{D} - \mathbf{P}$ is the Laplacian matrix. \mathbf{F} represents the learned graph embeddings of classes, which captures the co-occurrence information of each class. Its solution $\hat{\mathbf{F}}$ is the eigenvectors corresponding to the top- k minimum eigenvalues. By applying k -means on $\hat{\mathbf{F}}$, we divide the original label set into K subsets. For each labeled instance \mathbf{x}_i , we determine its context label c_i based on which subset its semantic labels belong to.

Semi-Supervised Context Identification. We formulate the context identification task as a semi-supervised learning problem, where we are given a labeled training set $\mathcal{D}_l^{aux} = \{(\mathbf{x}_i, c_i)\}_{i=1}^m$ and an unlabeled training set $\mathcal{D}_u^{aux} = \{\mathbf{x}_j\}_{j=1}^n$. Our target is to train a context identifier based on the labeled and unlabeled training examples, with the goal of boosting the performance of target multi-label alignment by exploiting contextual information.

For every instance \mathbf{x} , according to Eq. (3), we obtain the global features \mathbf{g} . Compared to the local features, the global features capture the global information, which is beneficial for identifying the context. Then, by feeding \mathbf{g} into a fully-connection layer and the softmax activation function, we obtain the predictions \mathbf{q}^a (for weakly-augmented version) and \mathbf{p}^a (for strongly-augmented version). For a unlabeled instances \mathbf{x}_j , we determine its pseudo-label \hat{c}_j based on the probability \mathbf{p}_j^a by $\hat{c}_j = \arg \max_k p_{jk}^a$. Then, we define the auxiliary loss, which comprises a supervised component

and an unsupervised component, as follows:

$$\mathcal{L}_{aux} = \sum_{i=1}^m L_{ce}(\mathbf{p}_i^a, c_i) + \sum_{j=1}^n \mathbf{1}(\max(\mathbf{q}_j^a) > \tau) L_{ce}(\mathbf{p}_j^a, \hat{c}_j), \quad (11)$$

where τ is the threshold to select reliable pseudo-labels [32], and L_{ce} is the cross entropy loss. Finally, we define the overall loss function as:

$$\mathcal{L} = \mathcal{L}_{sup} + \mathcal{L}_{unsup} + \mathcal{L}_{aux}. \quad (12)$$

In general, the target and auxiliary tasks improve the performance of SSMLL from two perspectives: 1) by performing semantic-aware alignment, we enhance the recognition ability of the model via effective label-specific feature extraction; 2) by designing the context identification auxiliary task, we enhance the learning of feature representations by leveraging co-occurrence information.

4. Experiment

4.1. Experiment Settings

Model Architecture. To ensure a fair comparison with other methods, we employ ResNet-50 [16] as the image encoder backbone of CLIP, and utilize the CLIP transformer as text encoder. Throughout training, the parameters of these two backbones remain frozen. We adopt the class-specific [48] setting for prompts, where each category possesses an independent set of parameters. We optimize two independent context vectors with 16 context tokens following [34]. To generate label-specific features, we use a transformer decoder consisting of 2 layers.

Datasets. To assess the effectiveness of our method, we perform experiments on MS-COCO-2014 (COCO for short) [23], VOC-2012 (VOC for short) [10], and NUS-WIDE (NUS for short) [7]. Further details about these datasets can be found in the appendix due to space limit. We adopt label proportions within the range of $p \in \{0.05, 0.10, 0.15, 0.20\}$, and randomly sample from the dataset to construct the labeled training set, while leaving the rest without any annotations.

Methods. To thoroughly validate the effectiveness of our method, we compare it with four groups of methods: 1) two MLL baseline methods that simply use BCE and ASL loss; 2) three methods from [40] that utilize instance-aware pseudo-labeling techniques; 3) one state-of-the-art SSMLL method CAP that uses class-wise thresholds to generate pseudo-labels; 4) four CLIP-based methods that fine-tune prompts to deal with partial labels. Note that for the last group of methods, we combine them with CAP to generate high-quality pseudo-labels.

Implementations Details. We employ the clustering method to partition the original label space into $K = 6$

Method	VOC				COCO			
	$p = 0.05$	$p = 0.10$	$p = 0.15$	$p = 0.20$	$p = 0.05$	$p = 0.10$	$p = 0.15$	$p = 0.20$
BCE	67.95	75.35	78.19	79.38	58.90	63.75	65.91	67.33
ASL	71.46	78.00	79.69	80.77	59.12	63.82	66.10	67.51
Top-1*	77.89	82.40	83.44	84.10	59.94	65.83	67.81	68.50
Top-k*	76.60	80.44	82.26	83.30	62.39	66.97	68.24	68.66
IAT*	75.00	77.63	81.67	82.77	62.93	66.18	67.46	68.56
CAP [40]	76.16	82.16	83.48	84.41	62.43	67.36	69.11	70.41
DualCoOp [34]	79.16	83.69	84.55	85.46	65.81	68.55	69.61	69.97
SCPNet [9]	78.03	78.70	79.68	80.30	61.00	62.11	62.49	62.81
TaI [15]	79.14	82.93	84.14	84.64	67.02	69.31	69.94	70.25
DualCoOp++ [17]	80.31	83.79	85.21	85.90	67.19	69.10	70.26	70.67
Ours	82.10	84.82	85.91	86.85	69.09	71.86	73.23	74.28

Table 1. **Comparison results on VOC and COCO in terms of mean Average Precision (mAP %).** We compare our approach with SOTA methods under MLMML problem setting and those methods based on fine-tuning CLIP. The best performance is highlighted in bold. Note that the symbol * denotes that combining DualCoOp [34] with different pseudo labeling methods.

Method	ASL	Top-1*	Top-k*	IAT*	CAP	DualCoOp	SCPNet	TaI	DualCoOp++	Ours
$p = 0.05$	42.87	39.39	41.48	42.78	44.82	46.92	47.12	48.90	47.19	50.21
$p = 0.10$	46.50	44.79	45.89	45.83	48.24	48.82	48.89	50.77	48.81	51.65
$p = 0.15$	48.42	46.65	47.63	47.44	49.90	49.94	49.52	51.88	50.10	53.01
$p = 0.20$	49.65	47.57	47.78	48.02	51.06	50.07	49.96	51.74	50.41	53.78

Table 2. **Comparison results on NUS in terms of mAP (%).** The best performance is highlighted in bold. Note that the symbol * denotes that combining DualCoOp [34] with different pseudo labeling methods.

CBSA			COCO				VOC			
TP	SAA	CI	$p = 0.05$	$p = 0.10$	$p = 0.15$	$p = 0.20$	$p = 0.05$	$p = 0.10$	$p = 0.15$	$p = 0.20$
			62.43	67.36	69.11	70.41	76.16	82.16	83.48	84.41
✓			67.02	69.31	69.94	70.25	79.14	82.93	84.14	84.64
✓	✓		68.65	71.39	72.96	73.91	80.40	84.15	85.67	86.79
✓	✓	✓	69.09	71.86	73.23	74.28	82.10	84.82	85.91	86.85

Table 3. **Ablation study.** Effects of different modules in our proposed method. We report the experiment results in terms of mAP (%) on COCO and VOC datasets. The best performance is displayed in bold.

clusters for MS-COCO, $K = 2$ for VOC, and $K = 2$ for NUS-WIDE. The optimization process utilizes AdamW optimizer and a one-cycle policy scheduler with a learning rate of $1e-3$. For all datasets, we set the number of warm-up epochs to 8, and the total epochs to 40. The batch sizes are configured as 8, 64, and 64 for VOC, COCO, and NUS respectively. Additionally, the threshold for semi-supervised context identification is set to 0.9. All experiments are conducted on NVIDIA 3090 with a fixed seed of 1.

4.2. Comparisons Results

Experimental results on VOC, COCO and NUS are presented in Table 1 and Table 2. From the tables, we can see that: 1) abundant knowledge embedded in VLMs like CLIP could effectively alleviate the challenge of limited labeled data in SSMLL. 2) Although DualCoOp and TaI also adopt a dual prompts design and utilize the same thresholding strategy to obtain pseudo-labels, the performance of our method are significantly better than them. 3) Our method achieves the best performance in all experimental settings and significantly outperforms other methods espe-



Figure 4. Visualization of images within various contexts that have top prediction probability.

cially under small labeled ratios without introducing much higher computational cost. The training cost of different methods is presented in the appendix. The performance improvement can be attributed to the introduction of auxiliary task and better feature representation with our semantic-aware alignment target task. This validates that simplifying alignment task into a one-to-one problem, *i.e.*, extracting label-specific image feature, is highly effective in dealing with multiple semantics in MLL. These experimental results demonstrate that our method exploits pre-training knowledge of CLIP more effectively.

4.3. Ablation Study

To comprehensively analyze the effect of different components in our method, we conducted an ablation study on COCO and VOC under various labeled ratio settings. As depicted in Table 3, each module of our method demonstrates a positive effect on performance. In comparison to the baseline method CAP, fine-tuning CLIP by merely incorporating a target prompt (TP) exhibits a notable performance boost, particularly under small labeled ratio setting. On COCO dataset, TP leads to a 6.66% mAP performance improvement when the ratio of labeled data $p = 0.05$. Additionally, semantic-aware alignment (SAA) demonstrates a more significant performance increase as the labeled ratio increases, with the increase of 3.50% and 2.15% in mAP under $p = 0.20$ on COCO and VOC respectively, which demonstrates that extracting label-specific feature from images leads to a better alignment between textual and visual modalities. With the introduction of the context identification auxiliary task, the performance further improves by an average of 0.67%, which validates that the introduction of this auxiliary task could help model obtain accurate over-

all understanding of an image. To further explore the effect of auxiliary task context identification, we adjust the number of clusters in context partition task. As shown in Table 4, our model achieves the best performance when context quantity $K = 6$.

To validate the generalization ability of our method, we also conduct experiments on other settings of multi-label learning. Due to the page limit, we present the experiment results in Appendix B.1.

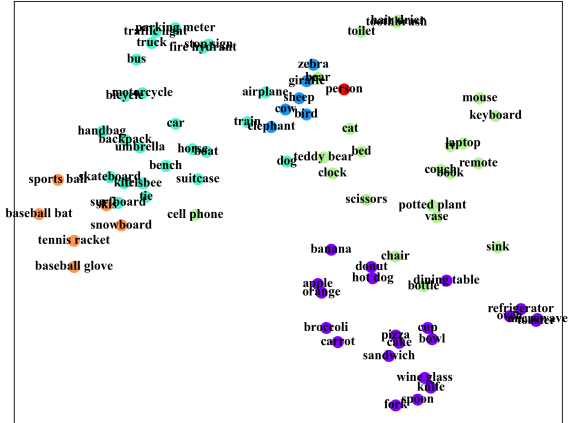


Figure 5. Context clusters generated by spectral clustering based on correlation matrix of COCO.

4.4. Further Analysis

In this section, we first present the clustering results of the COCO dataset using the correlation matrix of different categories. As depicted in Fig. 5, with the context count K set to 6 on COCO, the original label space is divided into

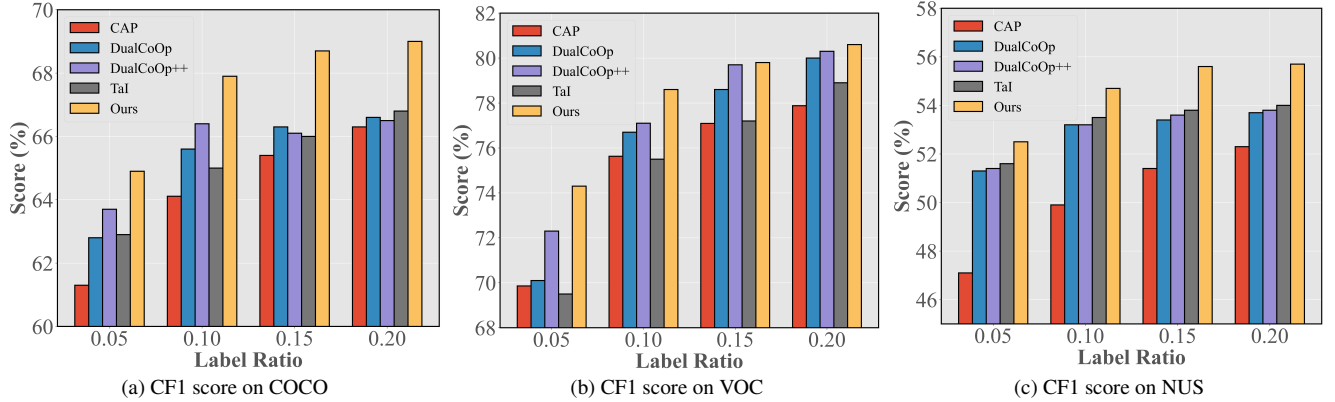


Figure 6. The quality of pseudo labels in terms of CF1 score on COCO, VOC and NUS.

# Context	COCO			
	$p = 0.05$	$p = 0.10$	$p = 0.15$	$p = 0.20$
$K = 1$	68.65	71.39	72.96	73.91
$K = 4$	69.01	71.69	73.20	74.25
$K = 6$	69.09	71.86	73.23	74.28

Table 4. The effect of different context quantity.

6 clusters. We can clearly observe that semantics that tend to co-occur are grouped into the same context. Based on the clustering results, we can partition the initial label space into 6 distinct subsets: *food*, *animals*, *sports*, *traffic*, *furniture*, and *people*.

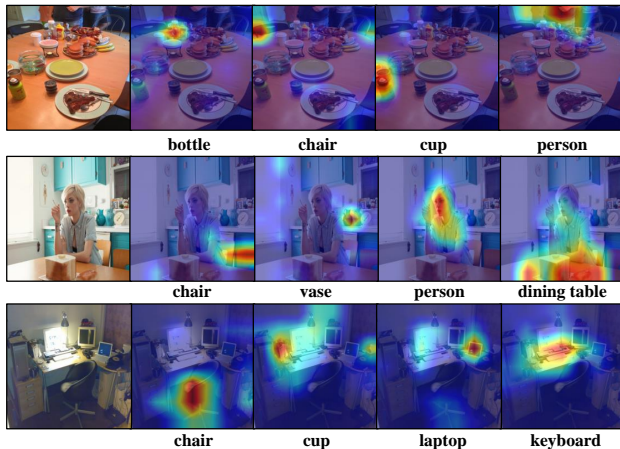


Figure 7. Visualization of different objects in COCO. Our model could effectively focus on the location of different semantics.

For a direct visualization of the context identification results, we employ our trained context classifier to select several images within each context with high confidence scores, as demonstrated in Fig. 4. From the result of context

classification, we can see that the result is closely aligned with the clustering result based correlation matrix estimated on labeled dataset. For instance, within the context of *food*, it is obvious that kitchens or tables are often present in the background of images belonging to this context, which means that with the introduction of context identification task, our method can effectively capture co-occurrence relationships, resulting in improved pseudo-labeling performance.

Furthermore, we evaluate the quality of pseudo labels in terms of CF1 score. Fig. 6 illustrates the result of CF1 scores on three datasets under different labeled ratios. We can clearly observe that our framework achieves the best performance under all labeled ratio settings, and achieves a more significant performance as the labeled ratio increases. This validates that our method could leverage supervised information more effectively and generate more accurate pseudo labels to boost the learning on unlabeled dataset.

In order to further demonstrate the model’s capability to locate various semantic information, we adopt CAM [29] technique to visualize where the model is placing its attention. As shown in Fig. 7, we can see that our model has a powerful ability to locate different semantics, including challenging targets like tiny objects, such as *cup* and *vase*. These results demonstrate that our method is able to significantly enhance the recognition ability of the model based on limited labeled data, resulting in favorable pseudo-labeling performance.

5. Conclusion

In this paper, we propose a novel framework to tackle the problem of semi-supervised multi-label learning, which is the first work that adapts vision-language model, *i.e.*, CLIP, under this problem setting. With the target of achieving better alignment between textual and visual modalities, we equip our model with semantic-aware prompts to extract label-specific image features. To incorporate the model with comprehensive understanding of image, we design a

new auxiliary task, context identification, which benefits the main classification task by exploiting co-occurrence relationships. Furthermore, we formulate context identification in a semi-supervised learning manner to extract more supervised information from limited labeled data, benefiting the learning process on unlabeled samples by enhancing the quality of pseudo-labels. Extensive experiments on multiple benchmarks have demonstrated that our method can achieve state-of-the-art performance. In the future, we will further study how to generalize our method into other problem settings, and align textual and visual modalities more closely to further increase model performance.

References

- [1] Dolly Carrillo, Vivian F López, and María N Moreno. Multi-label classification for recommender systems. In *Trends in Practical Applications of Agents and Multiagent Systems: 11th International Conference on Practical Applications of Agents and Multi-Agent Systems*, pages 181–188. Springer, 2013. 1
- [2] Haomin Chen, Shun Miao, Daguang Xu, Gregory D Hager, and Adam P Harrison. Deep hierarchical multi-label classification applied to chest x-ray abnormality taxonomies. *Medical image analysis*, 66:101811, 2020. 1, 2
- [3] Tianshui Chen, Muxin Xu, Xiaolu Hui, Hefeng Wu, and Liang Lin. Learning semantic-specific graph representation for multi-label image recognition. In *Proceedings of the IEEE/CVF international conference on computer vision*, pages 522–531, 2019. 1, 2
- [4] Tianshui Chen, Tao Pu, Hefeng Wu, Yuan Xie, and Liang Lin. Structured semantic transfer for multi-label recognition with partial labels. In *Proceedings of the AAAI conference on artificial intelligence*, pages 339–346, 2022. 1, 2
- [5] Tianshui Chen, Tao Pu, Lingbo Liu, Yukai Shi, Zhijing Yang, and Liang Lin. Heterogeneous semantic transfer for multi-label recognition with partial labels. *International Journal of Computer Vision*, 2024. 1, 2
- [6] Zhao-Min Chen, Xiu-Shen Wei, Peng Wang, and Yanwen Guo. Multi-label image recognition with graph convolutional networks. In *Proceedings of the IEEE/CVF conference on computer vision and pattern recognition*, pages 5177–5186, 2019. 2, 4, 1
- [7] Tat-Seng Chua, Jinhui Tang, Richang Hong, Haojie Li, Zhiping Luo, and Yantao Zheng. Nus-wide: a real-world web image database from national university of singapore. In *Proceedings of the ACM international conference on image and video retrieval*, pages 1–9, 2009. 5
- [8] Elijah Cole, Oisín Mac Aodha, Titouan Loré, Pietro Perona, Dan Morris, and Nebojsa Jojic. Multi-label learning from single positive labels. In *Proceedings of the IEEE/CVF Conference on Computer Vision and Pattern Recognition*, pages 933–942, 2021. 2
- [9] Zixuan Ding, Ao Wang, Hui Chen, Qiang Zhang, Pengzhang Liu, Yongjun Bao, Weipeng Yan, and Jungong Han. Exploring structured semantic prior for multi label recognition with incomplete labels. In *Proceedings of the IEEE/CVF Conference on Computer Vision and Pattern Recognition*, pages 3398–3407, 2023. 2, 3, 6, 1
- [10] Mark Everingham, SM Ali Eslami, Luc Van Gool, Christopher KI Williams, John Winn, and Andrew Zisserman. The pascal visual object classes challenge: A retrospective. *International journal of computer vision*, 111:98–136, 2015. 5
- [11] Peng Gao, Shijie Geng, Renrui Zhang, Teli Ma, Rongyao Fang, Yongfeng Zhang, Hongsheng Li, and Yu Qiao. Clip-adapter: Better vision-language models with feature adapters. *International Journal of Computer Vision*, pages 1–15, 2023. 3
- [12] Chunjiang Ge, Rui Huang, Mixue Xie, Zihang Lai, Shiji Song, Shuang Li, and Gao Huang. Domain adaptation via prompt learning. *arXiv preprint arXiv:2202.06687*, 2022. 2
- [13] Zongyuan Ge, Dwarikanath Mahapatra, Xiaojun Chang, Zetao Chen, Lianhua Chi, and Huimin Lu. Improving multi-label chest x-ray disease diagnosis by exploiting disease and health labels dependencies. *Multimedia Tools and Applications*, 79:14889–14902, 2020. 1
- [14] Hao Guo and Song Wang. Long-tailed multi-label visual recognition by collaborative training on uniform and re-balanced samplings. In *Proceedings of the IEEE/CVF Conference on Computer Vision and Pattern Recognition*, pages 15089–15098, 2021. 2
- [15] Zixian Guo, Bowen Dong, Zhilong Ji, Jinfeng Bai, Yiwen Guo, and Wangmeng Zuo. Texts as images in prompt tuning for multi-label image recognition. In *Proceedings of the IEEE/CVF Conference on Computer Vision and Pattern Recognition*, pages 2808–2817, 2023. 3, 6
- [16] Kaiming He, Xiangyu Zhang, Shaoqing Ren, and Jian Sun. Deep residual learning for image recognition. In *Proceedings of the IEEE conference on computer vision and pattern recognition*, pages 770–778, 2016. 4, 5
- [17] Ping Hu, Ximeng Sun, Stan Sclaroff, and Kate Saenko. Dualcoop++: Fast and effective adaptation to multi-label recognition with limited annotations. *arXiv preprint arXiv:2308.01890*, 2023. 6
- [18] Yusheng Huang, Jiexing Qi, Xinbing Wang, and Zhouhan Lin. Asymmetric polynomial loss for multi-label classification. In *ICASSP 2023-2023 IEEE International Conference on Acoustics, Speech and Signal Processing (ICASSP)*, pages 1–5. IEEE, 2023. 2
- [19] Menglin Jia, Luming Tang, Bor-Chun Chen, Claire Cardie, Serge Belongie, Bharath Hariharan, and Ser-Nam Lim. Visual prompt tuning. In *European Conference on Computer Vision*, pages 709–727. Springer, 2022. 2
- [20] Feng Kang, Rong Jin, and Rahul Sukthankar. Correlated label propagation with application to multi-label learning. In *2006 IEEE Computer Society Conference on Computer Vision and Pattern Recognition (CVPR'06)*, pages 1719–1726. IEEE, 2006. 1
- [21] Youngwook Kim, Jae Myung Kim, Zeynep Akata, and Jungwoo Lee. Large loss matters in weakly supervised multi-label classification. In *Proceedings of the IEEE/CVF Conference on Computer Vision and Pattern Recognition*, pages 14156–14165, 2022. 2

- [22] Jack Lanchantin, Tianlu Wang, Vicente Ordonez, and Yanjun Qi. General multi-label image classification with transformers. In *Proceedings of the IEEE/CVF Conference on Computer Vision and Pattern Recognition*, pages 16478–16488, 2021. 2
- [23] Tsung-Yi Lin, Michael Maire, Serge Belongie, James Hays, Pietro Perona, Deva Ramanan, Piotr Dollár, and C Lawrence Zitnick. Microsoft coco: Common objects in context. In *Computer Vision—ECCV 2014: 13th European Conference, Zurich, Switzerland, September 6–12, 2014, Proceedings, Part V 13*, pages 740–755. Springer, 2014. 5
- [24] Saravanapriya Manoharan, Radha Senthilkumar, and Saktheeswaran Jayakumar. Optimized multi-label convolutional neural network using modified genetic algorithm for popularity based personalized news recommendation system. *Concurrency and Computation: Practice and Experience*, 34(19):e7033, 2022. 1
- [25] Tao Pu, Tianshui Chen, Hefeng Wu, and Liang Lin. Semantic-aware representation blending for multi-label image recognition with partial labels. In *Proceedings of the AAAI Conference on Artificial Intelligence*, pages 2091–2098, 2022. 2, 1
- [26] Tao Pu, Tianshui Chen, Hefeng Wu, Yukai Shi, Zhijing Yang, and Liang Lin. Dual-perspective semantic-aware representation blending for multi-label image recognition with partial labels. *Expert Systems with Applications*, 249:123526, 2024. 1, 2
- [27] Yongming Rao, Wenliang Zhao, Guangyi Chen, Yansong Tang, Zheng Zhu, Guan Huang, Jie Zhou, and Jiwen Lu. Densclip: Language-guided dense prediction with context-aware prompting. In *Proceedings of the IEEE/CVF Conference on Computer Vision and Pattern Recognition*, pages 18082–18091, 2022. 3
- [28] Tal Ridnik, Emanuel Ben-Baruch, Nadav Zamir, Asaf Noy, Itamar Friedman, Matan Protter, and Lihi Zelnik-Manor. Asymmetric loss for multi-label classification. In *Proceedings of the IEEE/CVF International Conference on Computer Vision*, pages 82–91, 2021. 2, 4
- [29] Ramprasaath R Selvaraju, Michael Cogswell, Abhishek Das, Ramakrishna Vedantam, Devi Parikh, and Dhruv Batra. Grad-cam: Visual explanations from deep networks via gradient-based localization. In *Proceedings of the IEEE international conference on computer vision*, pages 618–626, 2017. 8
- [30] Sheng Shen, Shijia Yang, Tianjun Zhang, Bohan Zhai, Joseph E Gonzalez, Kurt Keutzer, and Trevor Darrell. Multitask vision-language prompt tuning. *arXiv preprint arXiv:2211.11720*, 2022. 2
- [31] Manli Shu, Weili Nie, De-An Huang, Zhiding Yu, Tom Goldstein, Anima Anandkumar, and Chaowei Xiao. Test-time prompt tuning for zero-shot generalization in vision-language models. *Advances in Neural Information Processing Systems*, 35:14274–14289, 2022. 2
- [32] Kihyuk Sohn, David Berthelot, Nicholas Carlini, Zizhao Zhang, Han Zhang, Colin A Raffel, Ekin Dogus Cubuk, Alexey Kurakin, and Chun-Liang Li. Fixmatch: Simplifying semi-supervised learning with consistency and confidence. *Advances in neural information processing systems*, 33:596–608, 2020. 5
- [33] Vladislav Sovrasov. Combining metric learning and attention heads for accurate and efficient multilabel image classification. *arXiv preprint arXiv:2209.06585*, 2022. 2
- [34] Ximeng Sun, Ping Hu, and Kate Saenko. Dualcoop: Fast adaptation to multi-label recognition with limited annotations. *Advances in Neural Information Processing Systems*, 35:30569–30582, 2022. 2, 3, 5, 6, 1
- [35] Bo Wang, Zhuowen Tu, and John K Tsotsos. Dynamic label propagation for semi-supervised multi-class multi-label classification. In *Proceedings of the IEEE international conference on computer vision*, pages 425–432, 2013. 2
- [36] Lichen Wang, Yunyu Liu, Can Qin, Gan Sun, and Yun Fu. Dual relation semi-supervised multi-label learning. In *Proceedings of the AAAI Conference on Artificial Intelligence*, pages 6227–6234, 2020. 2
- [37] Zhouxia Wang, Tianshui Chen, Guanbin Li, Ruijia Xu, and Liang Lin. Multi-label image recognition by recurrently discovering attentional regions. In *Proceedings of the IEEE international conference on computer vision*, pages 464–472, 2017. 2
- [38] Ming-Kun Xie and Sheng-Jun Huang. Partial multi-label learning. In *Proceedings of the AAAI conference on artificial intelligence*, 2018. 2
- [39] Ming-Kun Xie, Feng Sun, and Sheng-Jun Huang. Partial multi-label learning with meta disambiguation. In *Proceedings of the 27th ACM SIGKDD conference on knowledge discovery & data mining*, pages 1904–1912, 2021. 2
- [40] Ming-Kun Xie, Jia-Hao Xiao, Gang Niu, Masashi Sugiyama, and Sheng-Jun Huang. Class-distribution-aware pseudo labeling for semi-supervised multi-label learning. *arXiv preprint arXiv:2305.02795*, 2023. 4, 5, 6, 1
- [41] Jiazhi Xu, Sheng Huang, Fengtao Zhou, Luwen Huangfu, Daniel Zeng, and Bo Liu. Boosting multi-label image classification with complementary parallel self-distillation. *arXiv preprint arXiv:2205.10986*, 2022. 2, 4, 5
- [42] Vacit Oguz Yazici, Abel Gonzalez-Garcia, Arnau Ramisa, Bartłomiej Twardowski, and Joost van de Weijer. Orderless recurrent models for multi-label classification. In *Proceedings of the IEEE/CVF Conference on Computer Vision and Pattern Recognition*, pages 13440–13449, 2020. 2
- [43] Jin Yuan, Shikai Chen, Yao Zhang, Zhongchao Shi, Xin Geng, Jianping Fan, and Yong Rui. Graph attention transformer network for multi-label image classification. *ACM Transactions on Multimedia Computing, Communications and Applications*, 19(4):1–16, 2023. 2
- [44] Renrui Zhang, Wei Zhang, Rongyao Fang, Peng Gao, Kun-chang Li, Jifeng Dai, Yu Qiao, and Hongsheng Li. Tip-adapter: Training-free adaption of clip for few-shot classification. In *European Conference on Computer Vision*, pages 493–510. Springer, 2022. 3
- [45] Renrui Zhang, Xiangfei Hu, Bohao Li, Siyuan Huang, Hanqiu Deng, Yu Qiao, Peng Gao, and Hongsheng Li. Prompt, generate, then cache: Cascade of foundation models makes strong few-shot learners. In *Proceedings of the IEEE/CVF Conference on Computer Vision and Pattern Recognition*, pages 15211–15222, 2023. 3

- [46] Xin Zhang, Shixiang Shane Gu, Yutaka Matsuo, and Yusuke Iwasawa. Domain prompt learning for efficiently adapting clip to unseen domains. *arXiv preprint arXiv:2111.12853*, 2021. [2](#)
- [47] Feipeng Zhao and Yuhong Guo. Semi-supervised multi-label learning with incomplete labels. In *Twenty-fourth international joint conference on artificial intelligence*, 2015. [2](#)
- [48] Kaiyang Zhou, Jingkang Yang, Chen Change Loy, and Ziwei Liu. Learning to prompt for vision-language models. *International Journal of Computer Vision*, 130(9):2337–2348, 2022. [2](#), [3](#), [5](#), [1](#)

Context-Based Semantic-Aware Alignment for Semi-Supervised Multi-Label Learning

Supplementary Material

A. Experiment Settings

A.1. Details of Datasets

We conduct experiments on three benchmark datasets: MS-COCO-2014, VOC-2012, and NUS-WIDE. MS-COCO comprises a training set with 82,081 images and a test set with 40,137 images across 80 different classes. VOC-2012 consists of 5,717 images for training and 5,823 images for testing distributed among 20 classes. NUS-WIDE contains 150,000 images across 81 classes, featuring various resolutions for training, and 60,200 images for testing. These three datasets are widely used in SSMLL field to evaluate model performance. Compared with VOC, COCO and NUS have more semantics per image, which means that it's more challenging for model to correctly identify all objects in images.

A.2. Training Details

To ensure a fair comparison, we employ identical augmentation techniques across all methods, following the approach in [40]. Specifically, we apply both weak and strong augmentations to every image. Initially, each image is resized to 224×224 . For the weakly-augmented version, a random horizontal flip is performed. We adopt RandAugment and Cutout for the strongly-augmented version of image. We employ random initialization for learnable prompts in all CLIP-based methods and design class-specific prompts (CSP) following [48]. In this design, each class is associated with its own set of context tokens.

B. Additional Experiment Results

B.1. Performance on Partial Multi-label Setting

We conduct additional experiments on COCO in partial multi-label setting to further validate the effectiveness of our method, using the same experimental setup as in DualCoOP [34] and SCPNet [9] with ResNet-101 as the visual encoder of CLIP and all the images are resized into 448×448 . To create training samples with partial labels, we randomly mask out labels from complete annotation, and the proportion of available labels ranges from 10% to 80%.

In the partial multi-label setting, complete label annotations are unavailable, preventing us from obtaining an accurate co-occurrence matrix to leverage label correlations among categories and enhance the overall understanding of images. As a result, only the semantic-aware alignment module is used. We compare our method against two groups

of baselines: (1) six conventional partial multi-label learning methods, including SSGRL [3], GCN-ML [6], SST [4], SARB [25], HST [5], and DSRB [26]; (2) two methods based on fine-tuning learnable prompts in CLIP, namely, DualCoOP [34] and SCPNet [9]. As shown in Table 5, our method demonstrates improved performance as the proportion of available labels increases, indicating that extracting label-specific image features can achieve a more compact alignment between the two modalities.

Initialization	COCO			
	0.05	0.10	0.15	0.2
Random	69.09	71.86	73.23	74.28
Template	68.89	71.85	73.22	74.34

Table 6. Comparison of different initialization techniques. The best performance is displayed in bold (%).

B.2. Prompt Settings

Comparison of Initialization Techniques. We analyze the effect of different initialization techniques for prompts. Here, we compare the results of random initialization vs template initialization. For the template initialization, we construct a simple prompt template, *A photo of a [CLS]*, where [CLS] is replaced with actual class names. As depicted in Table 6, we observe similar performance with both initialization techniques. Thus different initialization methods have little effect on model's performance. So we simply use random initialization technique in all experiments.

Prompt Length	COCO			
	0.05	0.10	0.15	0.20
8	69.17	71.76	73.18	74.41
16	69.09	71.86	73.23	74.28
32	68.91	71.75	73.27	74.26
48	68.94	71.92	73.14	74.34
64	69.09	71.91	73.26	74.24

Table 7. The effect of prompt length. The best performance is displayed in bold (%).

Prompt Length. To investigate the effect of prompt length, we perform experiments with varying prompt length settings on the COCO dataset. The experimental results are

Dataset	Methods	10%	20%	30%	40%	50%	60%	70%	80%
COCO	SSGRL [3]	62.5	70.5	73.2	74.5	76.3	76.5	77.1	77.9
	GCN-ML [6]	63.8	70.9	72.8	74.0	76.7	77.1	77.3	78.3
	SST [4]	68.1	73.5	75.9	77.3	78.1	78.9	79.2	79.6
	SARB [25]	71.2	75.0	77.1	78.3	78.9	79.6	79.8	80.5
	HST [5]	70.6	75.8	77.3	78.3	79.0	79.4	79.9	80.2
	DSRB [26]	72.5	76.0	77.6	78.7	79.6	79.8	80.0	80.5
	DualCoOp [34]	78.7	80.9	81.7	82.0	82.5	82.7	82.8	83.0
	SCPNet [9]	80.3	82.2	82.8	83.4	83.8	83.9	84.0	84.1
	Ours (SAA)	79.8	81.9	83.5	84.3	84.4	84.7	85.0	85.3

Table 5. Comparison with methods in partial multi-label setting on COCO.

Prompt Setting	COCO			
	0.05	0.10	0.15	0.20
CSP	69.09	71.86	73.23	74.28
w/o CSP	68.93	71.52	72.96	74.13

Table 8. Comparison of different prompt setting. The best performance is displayed in bold (%).

presented in Table 7. Notably, the results demonstrate that different prompt lengths result in similar performance. This demonstrates that our method can achieve promising results without introducing high computational cost. In this case, we simply follow the same prompt length setting as in [34] to ensure the fairness.

Single vs Class-Specific Prompts. A single learnable prompt optimizes the same set of parameters across all classes, whereas the class-specific prompt (CSP) setting uses an individual set of optimizable parameters for each category. To discover the influence of prompt setting, we present the comparison result for these two approaches. As shown in Table 8, CSP consistently outperforms the single-prompt approach across all labeled settings on the COCO dataset, achieving a maximum improvement of 0.34%. This improvement demonstrates that optimizing the alignment between label-specific image features and class-specific text features effectively simplifies the original problem. Clearly, using independent prompts for each class enables a more effective alignment between the visual and textual modalities.

B.3. Computational Cost

We conduct additional experiments to compare the training cost of our method against baseline models. These experiments were performed on the COCO dataset under a $p = 0.05$ setting to evaluate the training efficiency of various approaches. As shown in Table 9, our method incurs

Methods	Training Latency (ms/img) ↓	Training Memory (GB/img) ↓	mAP (%) ↑
CAP	2.436	0.114	62.43
DualCoOp++	3.392	0.107	67.17
TaI	3.046	0.108	67.02
SCPNet	3.257	0.113	61.00
DualCoop	3.314	0.107	65.81
Ours	3.533	0.120	69.09

Table 9. Computational cost under $p = 0.05$ on COCO.

only a slight increase in training latency and VRAM usage while achieving significant performance gains under the $p = 0.05$ setting on COCO, which demonstrates that the introduction of semantic-aware alignment module and context identification task could achieve more compact alignment between visual and textual modalities and fully utilize contextual information to enhance feature representations.

B.4. Error Bars

In this section, we provide the error bar report on COCO dataset under different label ratios. We conduct 3 independent experiments with fixed random seeds 1, 2 and 3 respectively. And we choose 95% confidence interval and report standard error of the mean. As depicted in Table 10, our method demonstrates steady performance under all label ratio settings.

Methods	$p = 0.05$	$p = 0.10$	$p = 0.15$	$p = 0.20$
Ours	69.05±0.064	71.77±0.146	73.15±0.357	74.15±0.250

Table 10. Error bar report on COCO.